Combined analysis of MGMT methylation and dynamic-susceptibility-contrast MRI for the distinction between early and pseudo-progression in glioblastoma patients

A. Bani-Sadr, L.P. Berner, M. Barritault, L. Chamard, C.M. Bidet, O.F. Eker, M. Hermier, J. Guyotat, E. Jouanneau, D. Meyronet, et al.

Combined analysis of MGMT methylation and dynamic-susceptibility-contrast MRI for the distinction between early and pseudo-progression in glioblastoma patients.

Bani Sadr A[1], Berner LP[1], Barritault M[2,9], Chamard L[1], Bidet CM.[3], Eker OF[1,9], Hermier M[1], Guyotat J[4,9], Jouanneau E[5,8], Meyronet D[2,9], Gouttard S[6], D'Hombres A[7], Iziquierdo C[8], Honnorat J[8,9], Berthezène Y[1,9], Ducray F[8,9].

[1] Service de neuroradiologie, Groupe Hospitalier Est, Hospices de Civils de Lyon, 59 Bvd Pinel, 69634, Lyon Cedex, France.

[2] Service d'anatomopathologie, Groupe Hospitalier Est, Hospices Civils de Lyon, 59 Bvd Pinel, 69394, Lyon Cedex, France.

[3] Service de radiologie, Centre Hospitalier de Valence, 179 Bvd Juin, 26000, Valence, France

[4] Service de neurochirurgie D, Groupe Hospitalier Est, Hospices Civils de Lyon, 59 Bvd Pinel, 69634, Lyon Cedex, France.

[5] Service de neurochirurgie D, Groupe Hospitalier Est, Hospices Civils de Lyon, 59 Bvd Pinel, 69634, Lyon Cedex, France.

[6] Pôle d'activité médicale Imagerie, Hospices Civils de Lyon, 162 Av Lacassagne, 69424, Lyon Cedex, France.

[7] Service de radiothérapie, Centre Hospitalier Lyon Sud, 165 Chemin Du Grand Revoyet, 69310 Pierre-Bénite.

[8] Service de neuro-oncologie, Groupe Hospitalier Est, Hospices Civils de Lyon, 59 Bvd Pinel, 69394, Lyon Cedex, France.

[9] Université Claude Bernard Lyon 1, Lyon, France

Corresponding Author:

François Ducray,
Department of Neuro-Oncology,
Hôpital Neurologique de Lyon,
59 boulevard Pinel, 69394 Lyon Cedex, France,
Phone +(33) 4 72 35 78 06,
Fax +(33) 4 72 35 73 29,
e-mail : francois.ducray@chu-lyon.fr

Declarations of interest: none.

I. Abstract

I.1 Introduction

Currently, no single diagnostic modality allows the distinction between early progression (EP) and pseudo-progression (Psp) in glioblastoma patients. Herein we aimed to identify the characteristics associated with EP and Psp, and to analyze their diagnostic value alone and in combination.

I.2 Material and Methods

We reviewed the clinical, conventional magnetic resonance imaging (MRI), and molecular characteristics (*MGMT* promoter methylation, *IDH* mutation, and *EGFR* amplification) of glioblastoma patients who presented an EP (n= 59) or a Psp (n= 24) within six months after temozolomide radiochemotherapy. We analyzed relative cerebral blood volume (rCBV) and relative vessel permeability on K2 maps (rK2) in a subset of 33 patients using dynamic-susceptibility-contrast MRI.

I.3 Results

In univariate analysis, EP was associated with neurological deterioration, higher doses of dexamethasone, appearance of a new enhanced lesion, subependymal enhancement, higher rCBV and rK2 values. Psp occurred earlier after radiotherapy completion and was associated with *IDH1* R132H mutation, and *MGMT* methylation. In multivariate analysis, rCBV, rK2, and *MGMT* methylation status were independently associated with EP and Psp. All patients with a methylated *MGMT* promoter and a low rCBV (< 1.75) were classified as Psp while all patients with an unmethylated *MGMT* promoter and a high rCBV (≥ 1.75) were classified as EP. Among patients with discordant *MGMT* methylation and rCBV characteristics, higher rK2 values tended to be associated with EP.

I.4 Conclusion

Combined analysis of *MGMT* methylation, rCBV and vessel permeability on K2 maps seems helpful to distinguish EP from Psp. A prospective study is warranted to confirm these results.

I.5 Keywords:

Glioblastoma; Radiation injuries; Perfusion magnetic resonance imaging; Chemoradiotherapy; Disease Progression

I.6 Funding source:

This research did not receive any specific grant from funding agencies in the public, commercial, or not-profit sectors.

II. Manuscript.

II.1 Introduction:

Glioblastomas (GBM) are the most frequent primary brain tumors in adults. Their treatment consists of maximal surgical resection followed by radiotherapy with concurrent and adjuvant temozolomide (TMZ) [1]. Within six months after concurrent radiochemotherapy completion, up to 30% of patients develop new or worsening MRI contrast-enhancing lesions not resulting from early tumor progression (EP) but from radiation-induced changes [1]. This condition which mimics tumor progression has been termed pseudo-progression (Psp) and seems to be related to a radiation-induced increase of the permeability of the blood-brain barrier causing an increase in edema and contrast uptake [2,3]. Psp cannot reliably be distinguished from EP with conventional magnetic resonance imaging (MRI) [4]. The gold standard to differentiate EP and Psp is frequently considered to be new histological analysis. However, even at the neuropathological level, this distinction can be difficult because in a large proportion of patients with a suspicion of EP or Psp both tumor cells and post-radiation changes are found when a re-surgery is performed [5]. Therefore, the current recommendation in cases of suspected Psp is to continue TMZ and to conclude on Psp on a follow-up MRI if the contrast-enhancement improves or stabilizes and on EP if the contrast-enhancement worsens [5]. Thus, at present, the distinction between Psp and EP can only be made retrospectively, which has important implications for individual treatment.

Compared to Psp, several MRI characteristics have been associated with EP including more frequent subependymal contrast enhancement on conventional MRI [6,7], lower values of apparent diffusion coefficient (ADC) on diffusion weighted imaging (DWI) [7–10], higher relative cerebral blood volume (rCBV) on dynamic-susceptibility-contrast MRI (DSC-MRI)

[11–15], higher time-dependent leakage constant (Ktrans) on dynamic-contrast-enhanced MRI (DCE-MRI) [16,17] and higher choline/N-acetylaspartate ratios on magnetic resonance spectroscopy [18,19]. Metabolic imaging using positron emission tomography (PET) with 11C-methionine, 18F-fluorodopa and 18F-fluoro-ethyltyrosine has also been shown to be of interest in the differential diagnosis of Psp and EP [20,21]. At the molecular level, the presence of a methylated *MGMT* promoter and of an *IDH* mutation, which are associated with increased chemose nsitivity, has been shown to be associated with Psp [22–24]. Nevertheless, no single method has been validated for the differential diagnosis of EP or Psp, and it has been suggested that the optimal distinction between these conditions may be best achieved with the combination of several diagnostic modalities [25]. The aim of the present study was therefore to retrospectively identify clinical, radiological, and molecular characteristics associated with EP and Psp and to determine their diagnostic value, alone and in combination.

II.2 Methods:

II.2.1 Patient selection

Our institutional ethics committee approved this study. Patients were retrospectively identified in the radiological database of our establishment. They were included if they had histological diagnosis of GBM according to WHO 2016, were aged > 18 years-old, received TMZ radiochemotherapy as initial treatment, had radiological and clinical follow-up data available, and a radiological progression within six months after concurrent TMZ radiochemotherapy completion. Radiological progression was defined as any increase or new enhancement. Diagnoses of EP and Psp were made consensually by a neuro-oncologist and a radiologist blinded to molecular profiles. EP and Psp were diagnosed according to histological analysis or on follow-up MRI in the absence of treatment change. EP was diagnosed if follow-up MRI demonstrated an ongoing contrast-enhancement progression within six months after initial MRI worsening and Psp was diagnosed based on follow-up

MRI demonstrating contrast-enhancement stability or improvement within six months after initial radiological progression in the absence of treatment change.

II. 2.2 Clinical and molecular characteristics

The presence of a neurological deterioration (defined as the occurrence of any new neurological signs or the worsening of prior neurological signs), Karnofsky Performance Status (KPS), corticosteroid dosage at the time of Psp or EP, and date of death or last follow-up were collected from patients' medical files blinded to the final diagnosis. *MGMT* promoter methylation, *IDH*1R132H mutation and *EGFR* amplification status were collected from patient medical files and assessed as previously described [26]. They were available in 73, 70 and 54 patients, respectively.

II.2.3 MRI characteristics

MRI studies were obtained using 1.5T and 3T magnets. All studies included at least pre-contrast T1-weighted, T2-weighted, and fluid attenuation inversion recovery (FLAIR) images followed by DSC-MRI data when available and post-contrast T1-weighted images. Standard doses of 0.1mmol/kg gadolinium were used for contrast-enhanced images. The same dose of contrast agent was administered for both 1.5T and 3T scans.

DSC-MRI sequences were acquired using a gradient-echoplanner imaging (GE-EPI) technique during the first pass of a bolus of gadolinium contrast agent. The imaging parameters were as follows: time of repetition (TR) 2280 ms, time of emission (TE) 40 ms, flip angle 75°, matrix 212 x 136 mm slice thickness, no gap, 20 slices, field of view 224 mm, fat saturation, EPI factor 55. DSC-MRI were available in 33 patients (26 EP and 7 Psp).

MRI demonstrating worsening images were reviewed.

Two radiologists blinded to the final diagnosis identified the following signs on conventional sequences: appearance of a new enhanced lesion; marginal enhancement around the surgical cavity; nodular enhancement; callosal enhancement; subependymal enhancement;

meningeal enhancement; necrosis or cystic change; increased T2 peri-tumoral abnormality; decreasing of enhancement intensity; increasing cystic or necrosis change [6].

DSC-MRI were post-processed using Olea Sphere 3.0 software (Olea Medical. La Ciotat, France). Three, fixed-diameter (50-100 mm^2), regions of interest (ROI) were placed consensually by two radiologists in maximum areas for each CBV map and K2 map on tumor sites as previously described [27,28] and on healthy tissue in corona radiata to determine corrected rCBV and relative K2 (rK2) values. The ROI of maximum value was then selected for further analysis.

II.2.4 Statistical analysis

Descriptive analysis was conducted using Fischer's exact test. Logistic regression was applied to determine odds ratio (OR) of each variable in univariate and multivariate analysis. The multivariate model was built based on the analysis of all 33 patients with both DSC-MRI data and *MGMT* promoter methylation status available. For conventional MRI data, inter-rater agreement was determined by calculating Kappa coefficients following Landis and Koch guidelines. For DSC-MRI data, rCBV threshold was set at 1.75 because this is the most commonly accepted [13–15]. Optimal cut-off of rK2 was determined using receiver operation curve (ROC) by maximizing the Youden index. Overall survivals (OS) were determined from the date of the first surgery. They were computed using the Kaplan-Meier method and compared using the Log-rank test.

A diagnostic score combining rCBV ≥ 1.75, rK2 optimal threshold, and *MGMT* promoter status was constructed. Combination score was calculated for each patient with complete data (n= 33). The area under curve (AUC) of rCBV ≥ 1.75, rK2 optimal threshold, *MGMT* promoter status and the combined diagnostic score were computed and compared using the DeLong test. Statistical significance was set at $p< 0.05$. All analyses were conducted using R

software (R Core Team (2016). R: A language and environment for statistical computing. R Foundation for Statistical Computing, Vienna, Austria.).

II.3 Results:

From January 2005 to July 2016, we retrospectively identified 168 GBM patients who received TMZ radiochemotherapy and for whom radiological follow-up was available (the STARD diagram is shown in Figure 1). Of these patients, 105 (62%) showed radiological progression within six months after concurrent TMZ radiochemotherapy completion which corresponded to an EP in 59 patients (35%) and to a Psp in 24 patients (15%). In 22 patients, the distinction between EP and Psp was not possible because of early treatment change and these patients were excluded from further analysis. EP was diagnosed based on histological analysis obtained at the time of resurgery in four patients and in 55 patients based on follow-up MRI. Psp was diagnosed based on MRI follow-up in all patients. The median OS was statistically significantly longer ($p< 0.001$) in patients with Psp (39.5 months, 95% CI [36.4; 43.2]) than in those with EP (16.1 months, 95% CI [14.6; 17.3]; Figure 2). Characteristics of assessable patients and univariate analysis results can be found in Table 1 and in the supplementary Table. In univariate analysis, EP was associated with neurological deterioration (OR= 1.30, 95% CI [1.08; 1.58]), higher dose of dexamethasone (OR= 1.02, 95% CI [1.01; 1.03]), appearance of a new enhanced lesion (OR= 1.32, 95% CI [1.09; 1.60]), subependymal enhancement (OR= 1.29, 95% CI [1.07; 1.56]), higher rCBV (OR= 1.24, 95% CI [1.10; 1.41]), and higher rK2 (OR= 1.01, 95% CI [1.01; 1.02]) values. Psp occurred earlier after radiochemotherapy completion compared to EP (2.02 vs. 3.22 months, p= 0.012). Among Psp patients, the radiologic progression occurred within three months after radiochemotherapy completion in 18 out of 24 (75%) patients. Psp was associated with *IDH1* R132H mutation (OR= 2.04, 95% CI [1.08; 3.85]) as well as with the presence of a

methylated *MGMT* promoter (OR= 1.59, 95% CI [1.32; 1.92]). Optimal cut-off of rK2 was found at 27. The three characteristics with the highest diagnostic value were an rCBV ≥ 1.75 (92.3% sensitivity and 71.4% specificity for the diagnosis of EP) an rK2 ≥ 27 (76.9% sensitivity and 85.7% specificity for the diagnosis of EP) and a methylated *MGMT* promoter (100% sensitivity and 78% specificity for the diagnosis of Psp).

In multivariate analysis, only a rCBV ≥ 1.75 (OR= 1.44, 95% CI [1.16; 1.63), p< 0.001), a rK2 ≥ 27 (OR= 1.25, 95% CI [1.07; 1.46], p= 0.006) and a methylated *MGMT* promoter (OR= 1.29 95% CI [1.10; 1.52], p= 0.002) were independently associated with EP and Psp. Among the 33 patients in whom these characteristics were available, all four patients (12%) with a methylated *MGMT* promoter and a low rCBV (< 1.75) were classified as Psp while all 16 patients (48%) with an unmethylated *MGMT* promoter and a high rCBV were classified as EP. In the 13 patients (40%) in whom *MGMT* promoter methylation and rCBV were discordant (i.e. methylated *MGMT* promoter and high rCBV, or unmethylated *MGMT* promoter and low rCBV), seven out of the eight patients with a high rK2 (≥ 27) had an EP compared to three out of the five patients with a low rK2 (p= 0.5). Classification of these 33 patients with complete data can be found in table 2. Two examples illustrating potential interest of K2 maps can be found in figure 3. As shown in Figure 4, the area under the curve (AUC) score of the combined analysis of rCBV, rK2 and *MGMT* promoter methylation (0.94, 95% CI [0.92; 1]) was significantly greater than individual AUC score of rCBV≥ 1.75 (0.82, 95 CI [0.68; 0.86]), *MGMT* promoter methylation alone (0.77, 95% CI [0.67; 0.87]) and rK2≥ 27 (0.74, 95% CI [0.69; 0.80]). The AUC score of the combined analysis of rCBV, rK2 and *MGMT* promoter methylation was also better than the AUC score of the combined analysis of rCBV and MGMT promoter methylation status only (0.90, 95% CI [0.76-0.98]).

II.4 Discussion

Despite significant efforts to develop diagnostic tools, there is currently no validated method to distinguish EP from Psp, and the interpretation of MRI within six months after radiotherapy completion remains an everyday problem in the treatment of GBM patients. The present study suggests that combining the analysis of *MGMT* methylation with DSC-MRI, two widely available diagnostic methods in the clinical setting, could be helpful and warrant prospective evaluation.

Given that there is no gold standard to distinguish EP from Psp and that only a few patients in our series underwent pathological confirmation, we cannot exclude that, based on MRI follow-up alone, we misclassified some patients. However, the much longer OS observed in Psp compared to EP patients, strongly supports that our classification of Psp and EP patients was valid in most cases. In agreement with previous studies we found that EP and Psp were associated with different clinical, radiological, and molecular characteristics (Table 3). EP has been associated with neurological deterioration [29], subependymal contrast-enhancement [6,7], higher rCBV values [11–15], and higher vessel permeability [16,17]. In contrast, Psp was associated with *MGMT* methylation, *IDH* mutation, shorter delay after radiochemotherapy completion and longer OS [22–24].

Although several studies have focused on specific molecular and imaging characteristics, only a few have sought to identify the characteristics associated independently with these conditions [6,30] and, to our knowledge, no study has thoroughly analyzed their clinical, radiological, and molecular characteristics. Herein, based on a complete analysis of EP and Psp characteristics, we found that *MGMT* methylation, rCBV and rK2 had a higher diagnostic

value than clinical or conventional MRI characteristics and were independently associated with EP and Psp. The independent diagnostic value of *MGMT* methylation and perfusion imaging parameters is consistent with two previous studies indicating that the predictive value of rCBV varies with *MGMT* methylation [31] and that the combination of *MGMT* methylation with perfusion parameters may improve the diagnostic accuracy for Psp [12]. In the present study, the combination of *MGMT* methylation and rCBV analysis successfully classified patients in whom these characteristics were consistent; all patients with a methylated *MGMT* promoter and low rCBV values were classified as Psp, while all patients with an unmethylated *MGMT* promoter and high rCBV values were classified as EP. However, nearly half of patients had discordant characteristics (*MGMT* methylation and high rCBV, or absence of *MGMT* methylation and low rCBV) and could not be accurately classified. Consistent with these results, in a recent study based on DCE-MRI, 22 out of 23 patients (96%) with a methylated *MGMT* promoter and low normalized CBV values were classified as Psp while all 17 patients (100%) with an unmethylated *MGMT* promoter and high normalized CBV values were classified as EP [12]. In this study, the rate of discordance between *MGMT* methylation and rCBV characteristics was 60% [12] and in this situation, as herein, EP and Psp could not be accurately predicted. These findings suggest that, although combining *MGMT* methylation and rCBV analysis seems promising, additional information is needed to classify patients with discordant status.

To the best of our knowledge, the present study is the first to analyze the diagnostic value of DSC-MRI vessel permeability K2 maps for the distinction between EP and Psp. The reference perfusion MRI technique to assess vessel permeability in brain tumors is DCE-MRI [32]. Unlike DSC-MRI which is based on the first pass of a bolus of contrast media, DCE-MRI relies on the acquisition of serial T1-weighted images before, during, and after injection [33]. The resulting signal intensity-time curve reflects tissue perfusion, vessel permeability, and

interstitial space. From this data, the transfer constant, Ktrans can be derived [33]. In brain tumors, Ktrans has been shown to confidently reflect vessel permeability and to be an interesting tool to monitor treatment efficacy, namely after radiochemotherapy completion [16,17,32]. However, DCE-MRI image acquisition and post-processing is more complex than DSC-MRI and is therefore not easy to use in routine. K2 maps have been developed to allow the assessment of vessel permeability using DSC-MRI and K2 has been shown to correlate with Ktrans in gliomas [34]. Herein, consistent with DCE-MRI studies that have reported higher vessel permeability was predictive of EP [16,17] we observed that higher rK2 predicted EP, although with a lower sensitivity and specificity than rCBV. Interestingly, we found that rK2 diagnostic value was independent of rCBV, suggesting that the assessment of vessel permeability may further improve the diagnostic accuracy DSC-MRI. As suggested in the present study, K2 maps may be helpful in patients with discordant *MGMT* and rCBV status given that in these patients we observed that all but one patient with high K2 values were classified as EP. DSC-MRI has the advantage to be a widely available technique. However, an issue in daily practice is quite a high variability of rCBV assessment. In order, to limit this issue in the present study, rCBV measurements were made by two operators on a consensual basis. This strategy however prevented the analysis of inter-rater agreement for rCBV and rK2 analysis.

The present study has several limitations. In addition to its retrospective design, the number of patients with an available DSC-MRI was small and therefore the number of patients included in the multivariate analysis was limited. Furthermore, the distribution of Psp and EP patients included in the multivariate analysis was asymmetric. Although, DSC-MRI post-processing was centralized, one cannot exclude that MRI acquisition on 1.5T and 3T magnets may have resulted in bias in the subsequent analysis and radiological analysis included only conventional MRI, rCBV, and rK2.

Furthermore, molecular analysis did not include *TERT* promoter mutation which may modulate the prognostic value of *MGMT* methylation [35]. In line with previous reports, we found IDH1 R123H mutation to be associated with Psp but these results should be considered with caution as this mutation was only present in two patients, both in the Psp group [22, 23]. Beside these limitations, our study provides evidence that combined analysis of *MGMT* methylation and DSC-MRI may be a promising and simple strategy to better distinguish EP from Psp. A prospective study is warranted to confirm these results.

II.5 References:

[1] Weller M, van den Bent M, Tonn JC, Stupp R, Preusser M, Cohen-Jonanthan-Moyal E et al. European Association for Neuro-Oncology (EANO) guideline on the diagnosis and treatment of adults astrocytic and oligodendroglial gliomas. Lancet Oncol 2017; 18:e315-e29.

[2] Brandsma D, Stalpers L, Taal W, Sminia P, van den Bent MJ. Clinical features, mechanisms, and management of pseudoprogression in malignant gliomas. Lancet Oncol 2008; 9(5):453–461.

[3] Wick W, Chinot OL, Bendszus M, Masson W, Henriksson R, Saran F et al. Evaluation of pseudoprogression rates and tumor progression patterns in a phase III trial of bevacizumab plus radiotherapy/temozolomide for newly diagnosed glioblastoma. Neuro-Oncol 2016; 18(10):1434–1441.

[4] Van Den Bent MJ, Vogelbaum MA, Wen PY, Macdonald DR, Chang SM. End point assessment in gliomas: novel treatments limit usefulness of classical Macdonald's Criteria. J Clin Oncol 2009; 27(18):2905–2908.

[5] Melguizo-Gavilanes I, Bruner JM, Guha-Thakurta N, Hess KR, Puduvalli VK. Characterization of pseudoprogression in patients with glioblastoma: is histology the gold standard? J Neurooncol 2015; 123(1):141–150.

[6] Young RJ, Gupta A, Shah AD, Graber JJ, Zhang Z, Shi W et al. Potential utility of conventional MRI signs in diagnosing pseudoprogression in glioblastoma. Neurology 2007; 76(22):1918–1924.

[7] Yoo RE, Choi SH, Kim TM, Lee SH, Park CK, Park SH et al. Independent Poor Prognostic Factors for True Progression after Radiation Therapy and Concomitant Temozolomide in Patients with Glioblastoma: Subependymal Enhancement and Low ADC Value. Am J Neuroradiol 2015; 36(10):1846–1852.

[8] Reimer C, Deike K, Graf M, Reimer P, Wiestler B, Omar R et al. Differentiation of pseudoprogression and real progression in glioblastoma using ADC parametric response maps. PLOS one 2017; 12(4):e0174620.

[9] Prager AJ, Martinez N, Beal K, Omuro A, Zhang Z, Young RJ. Diffusion and Perfusion MRI to Differentiate Treatment-Related Changes Including Pseudoprogression from Recurrent Tumors in High-Grade Gliomas with Histopathologic Evidence. Am J Neuroradiol 2015; 36(5):877–885.

[10] Cha J, Kim ST, Kim HJ, Kim YK, Lee JY, Jeon P et al. Differentiation of Tumor Progression from Pseudoprogression in Patients with Posttreatment Glioblastoma Using Multiparametric Histogram Analysis. Am J Neuroradiol 2014; 35(7):1309–1317.

[11] Patel P, Baradaran H, Delgado D, Askin G, Christos P, Tsiouris A et al. MR perfusion-weighted imaging in the evaluation of high-grade gliomas after treatment: a systematic review and meta-analysis. Neuro-Oncol 2017; 19(1):118–127.

[12] Yoon RG, Kim HS, Paik W, Shim WH, Kim SJ, Kim JH. Different diagnostic values of imaging parameters to predict pseudoprogression in glioblastoma subgroups stratified by MGMT promoter methylation. Eur Radiol 2017; 27(1):255–266.

[13] Gahramanov S, Muldoon LL, Varallyay CG, Xin L, Kraemer DF, Fu R et al. Pseudoprogression of glioblastoma after chemo-and radiation therapy: diagnosis by using dynamic susceptibility-weighted contrast-enhanced perfusion MR imaging with ferumoxytol versus gadoteridol and correlation with survival. Radiology 2013; 266(3):842–852.

[14] Hu LS, Eschbacher JM, Heiserman JE, Dueck AC, Shapiro WR, Liu S et al. Reevaluating the imaging definition of tumor progression: perfusion MRI quantifies recurrent glioblastoma tumor fraction, pseudoprogression, and radiation necrosis to predict survival. Neuro-Oncol 2012; 14(7):919–930.

[15] Nasseri M, Gahramanov S, Netto JP, Fu R, Muldoon LL, Varallyay C et al. Evaluation of pseudoprogression in patients with glioblastoma multiforme using dynamic magnetic resonance imaging with ferumoxytol calls RANO criteria into question. Neuro-Oncol 2014; 16(8):1146–1154.

[16] Thomas AA, Arevalo-Perez J, Kaley T, Lyo J, Peck KK, Shi W et al. Dynamic contrast enhanced T1 MRI perfusion differentiates pseudoprogression from recurrent glioblastoma. J Neurooncol 2015; 125(1):183–190.

[17] Yun TJ, Park CK, Kim TM, Lee SH, Kim JH, Sohn CH et al. Glioblastoma treated with concurrent radiation therapy and temozolomide chemotherapy: differentiation of true progression from pseudoprogression with quantitative dynamic contrast-enhanced MR imaging. Radiology 2015; 274(3):830–840.

[18] Kazda T, Bulik M, Pospisil P, Lakomy R, Smrcka M, Slampa P et al. Advanced MRI increases the diagnostic accuracy of recurrent glioblastoma: Single institution thresholds

and validation of MR spectroscopy and diffusion weighted MR imaging. NeuroImage Clin 2016; 11:316–321.

[19] Shim H, Holder CA, Olson JJ. Magnetic resonance spectroscopic imaging in the era of pseudoprogression and pseudoresponse in glioblastoma patient management. CNS Oncol 2013; 2(5):393–396.

[20] Galldiks N, Langen KJ, Pope WB. From the clinician's point of view - What is the status quo of positron emission tomography in patients with brain tumors? Neuro-Oncol 2015; 17(11):1434–1444.

[21] Galldiks N, Dunkl V, Stoffels G, Hutterer M, Rapp M, Sabel M et al. Diagnosis of pseudoprogression in patients with glioblastoma using O-(2-[18F]fluoroethyl)-l-tyrosine PET. Eur J Nucl Med Mol Imaging 2015; 42(5):685–695.

[22] Li H, Li J, Cheng G, Zhang J, Li X. IDH mutation and MGMT promoter methylation are associated with the pseudoprogression and improved prognosis of glioblastoma multiforme patients who have undergone concurrent and adjuvant temozolomide-based chemoradiotherapy. Clin Neurol Neurosurg 2016; 151:31–36.

[23] Motegi H, Kamoshima Y, Terasaka S, Kobayashi H, Yamaguchi S, Tanino M et al. IDH1 mutation as a potential novel biomarker for distinguishing pseudoprogression from true progression in patients with glioblastoma treated with temozolomide and radiotherapy. Brain Tumor Pathol 2016; 30(2):67–72.

[24] Brandes AA, Franceschi E, Tosoni A, Blatt V, Pession A, Tallini G et al. *MGMT* Promoter Methylation Status Can Predict the Incidence and Outcome of Pseudoprogression After Concomitant Radiochemotherapy in Newly Diagnosed Glioblastoma Patients. J Clin Oncol 2008; 26(13):2192–2197

[25] Hyare H, Thust S, Rees J. Advanced MRI Techniques in the Monitoring of Treatment of Gliomas. Curr Treat Options Neurol 2017; 19(3)

[26] Meyronet D, Esteban-Mader M, Bonnet C, Joly MO, Uro-Coste E, Amiel-Benouaich A et al. Characteristics of H3 K27M-mutant gliomas in adults. Neuro-Oncol 2017; 19(8):1127–1134.

[27] Young RJ, Gupta A, Shah AD, Graber JJ, Chan TA, Zhang Z et al. MRI perfusion in determining pseudoprogression in patients with glioblastoma. Clin Imaging 2013; 37(1):41–49.

[28] Wetzel SG, Cha S, Johnson G, Lee P, Law M Kasow DL et al. Relative Cerebral Blood Volume Measurements in Intracranial Mass Lesions: Interobserver and Intraobserver Reproducibility Study. Radiology 2002; 224(3):797–803.

[29] Taal W, Brandsma D, de Bruin HG, Bromberg JE, Swaak-Kragten AT, Smitt PA et al. Incidence of early pseudo-progression in a cohort of malignant glioma patients treated with chemoirradiation with temozolomide. Cancer 2008; 113(2):405–410.

[30] Park HH, Roh TH, Kang SG, Kim EH, Hong CK, Kim SH et al. Pseudoprogression in glioblastoma patients: the impact of extent of resection. J Neurooncol 2016; 126(3):559–566.

[31] Kong DS, Kim ST, Kim EH, Lim DH, Kim WS, Suh YL et al. Diagnostic Dilemma of Pseudoprogression in the Treatment of Newly Diagnosed Glioblastomas: The Role of Assessing Relative Cerebral Blood Flow Volume and Oxygen-6-Methylguanine-DNA Methyltransferase Promoter Methylation Status. Am J Neuroradiol 2011; 32(2):382–387.

[32] Jackson A, Jayson GC, Li KL, Zhu XP, Checkley DR, Tessier JJ et al. Reproducibility of quantitative dynamic contrast-enhanced MRI in newly presenting glioma. Br J Radiol 2003; 76(903):153–162.

[33] Essig M, Shiroishi MS, Nguyen TB, Saake M, Provenzale JM, Enterline D et al. Perfusion MRI: The Five Most Frequently Asked Technical Questions. Am J Roentgenol 2013; 200(1):24–34.

[34] Taoka T, Kawai H, Nakane T, Hori S, Ochi T, Miyasaka Tet al. Application of histogram analysis for the evaluation of vascular permeability in glioma by the K2 parameter obtained with the dynamic susceptibility contrast method: Comparisons with Ktrans obtained with the dynamic contrast enhance method and cerebral blood volume. Magn Reson Imaging 2016; 34(7):896–901.

[35] Arita H, Yamasaki K, Matsushita Y, Nakamura T, Shimokawa A, Takami H et al. A combination of TERT promoter mutation and MGMT methylation status predicts clinically relevant subgroups of newly diagnosed glioblastomas. Acta Neuropathol Commun 2016; 4(1).

III. Appendices

III.1. Figure 1: STARD diagram.

STARD diagram reporting flow of participants through the study.

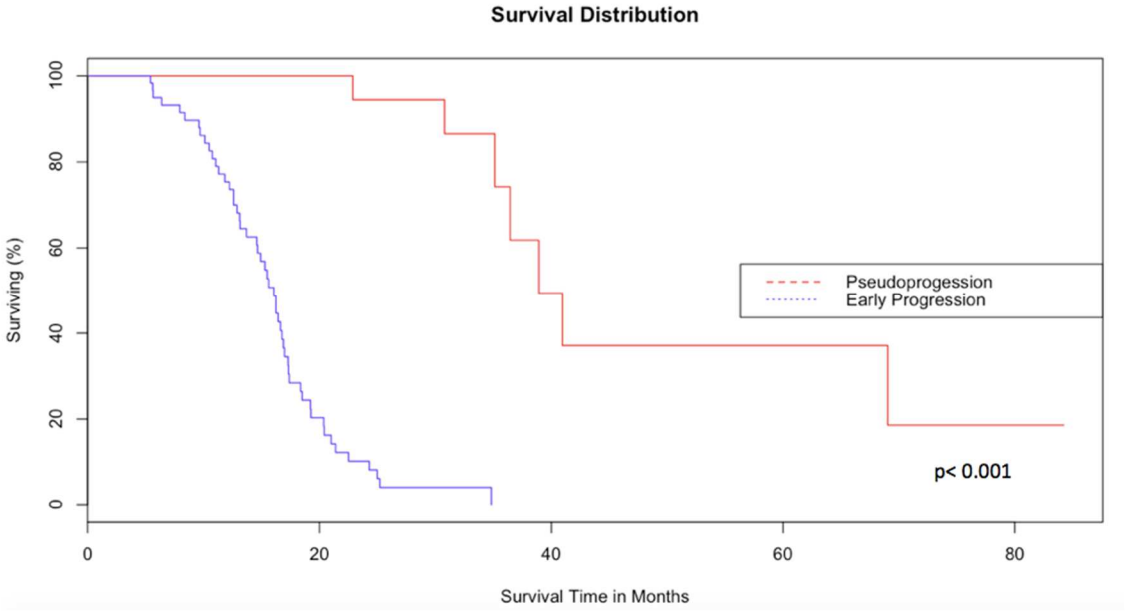

III.2 Figure 2: Survival of patients with early progression or pseudoprogression.

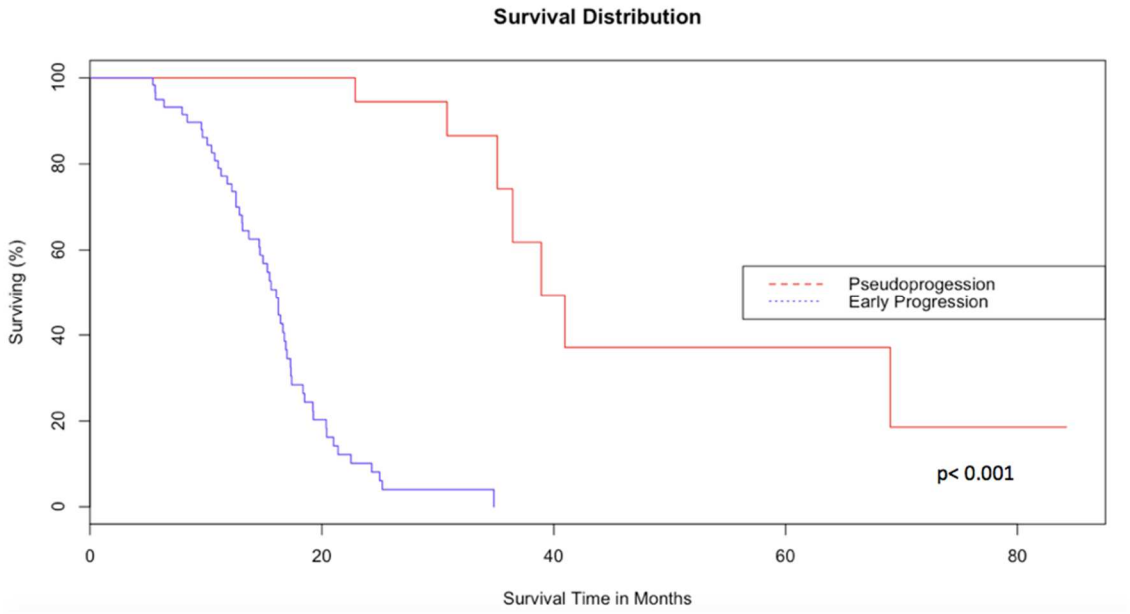

Survival of patients with early pseudoprogression are displayed in Kaplan-Meier curves.

Survival was significantly longer for patients with pseudoprogression (p-value < 0.001).

III.3. Table 1: Univariate analysis

	Psp	EP	OR [95% CI]	p-value*	Kappa coefficient
Clinical characteristics					
Age (year)	58.83 ± 9.64	54.83 ± 12.43	1.00 [0.99; 1.01]	0.120	
Sex			1.09 [0.89; 1.34]	0.391	
Female	11 (45.83%)	21 (35.59%)			
Male	13 (54.17%)	38 (64.41%)			
Extent of surgery					
Biopsy	10 (41. 67%)	27 (45. 77%)	1.03 [0.85; 1.26]	0.737	
Subtotal resection	7 (29. 16%)	11 (18.64%)	0.88 [0.69; 1.12]	0.297	
Gross total resection	7 (29. 16%)	21 (35.59%)	1.06 [0.86; 1.31]	0.580	
Delay after radiochemotherapy completion (months)	2.02 ± 1.74	3.22 ± 2.42	1.21 [1.14; 1.26]	0.012	
Karnofsky Performans status	76.3 ± 9.7	74.1 ± 12.8	0.99 [0.99; 1.02]	0.453	
Doses of dexamethasone (mg/d)	3.9 ± 6.1	6.9 ± 4.8	1.02 [1.01;1.03]	0.034	
Neurological deterioration	5 (20.83%)	31 (52.54%)	1.30 [1.08; 1.58]	0.008	
Conventional MRI characteristics					
New enhanced lesion	10 (41.67%)	43 (72.88%)	1.32 [1.09; 1.60]	0.007	0.92
Marginal enhancement	13 (54.17%)	29 (49.15%)	0.97 [0.80; 1.19]	0.787	0.97
Nodular enhancement	19 (79.17%)	55 (93.22%)	1.34 [0.99; 1.84]	0.063	0.84
Callosal enhancement	5 (20.83%)	20 (33.89%)	1.14 [0.92; 1.41]	0.245	0.88
Subependymal enhancement	6 (25.00%)	33 (55.93%)	1.29 [1.07; 1.56]	0.010	0.90
Meningeal enhancement	9 (37.50%)	25 (42.37%)	1.04 [0.85; 1.27]	0.687	0.94
Necrosis or cystic change	17 (70.83%)	50 (84.75%)	1.22 [0.96; 1.54]	0.103	0.93
Increased of T2 peri-tumoral abnormality	18 (75.00%)	52 (88.14%)	1.23 [0.94; 1.61]	0.139	0.88
Decrease of enhancement intensity	1 (4.17%)	2 (3.39%)	1.34 [0.54; 3.30]	0.527	0.48
Increasing necrosis or cystic change	14 (58.33%)	43 (72.88%)	1.04 [0.84; 1.29]	0.688	0.65
DSC-MRI characteristics**					
rCBV≥ 1.75	2 (28.57%)	24 (92.31%)	1.89 [1.44; 2.48]	< 0.001	
rK2≥ 27	1 (14.28%)	20 (76.92%)	1.57 [1.22; 2.03]	< 0.001	
rCBV	1.71 ± 0.47	2.95 ± 0.92	1.24 [1.10; 1.41]	0.002	
rK2	19.26 ± 10.01	37.03 ± 14.53	1.01 [1.01; 1.02]	0.004	
Molecular characteristics***					
Methylated *MGMT* promoter	18 (81.82%)	14 (27.4%)	0.63 [0.52; 0.76]	< 0.001	

*IDH*1 R132H mutation	2 (9.09%)	0 (0.00%)	0.49 [0.26; 0.93]	0.032
EGFR amplification	8 (36.36%)	17 (54.8%)	0.99 [0.79; 1.25]	0.940

* p-value estimated using logistic regression.

Notes. Unless otherwise indicated, continuous data are displayed by their means ± standard deviation and binary data are displayed by count numbers and frequencies (%). *MGMT* promoter methylation, *IDH*1R132H mutation and *EGFR* amplification status were available in 73, 70 and 54 patients, respectively.

Abbreviations: EP= early progression, Psp= pseudoprogression, OR= odds ratio, DSC-MRI= dynamic-susceptibility-contrast MRI, rCBV= relative cerebral blood volume, rK2= relative K2.

III.4. Figure 3: Illustrative examples of potential interest of K2 maps in discrimination of early and pseudoprogression.

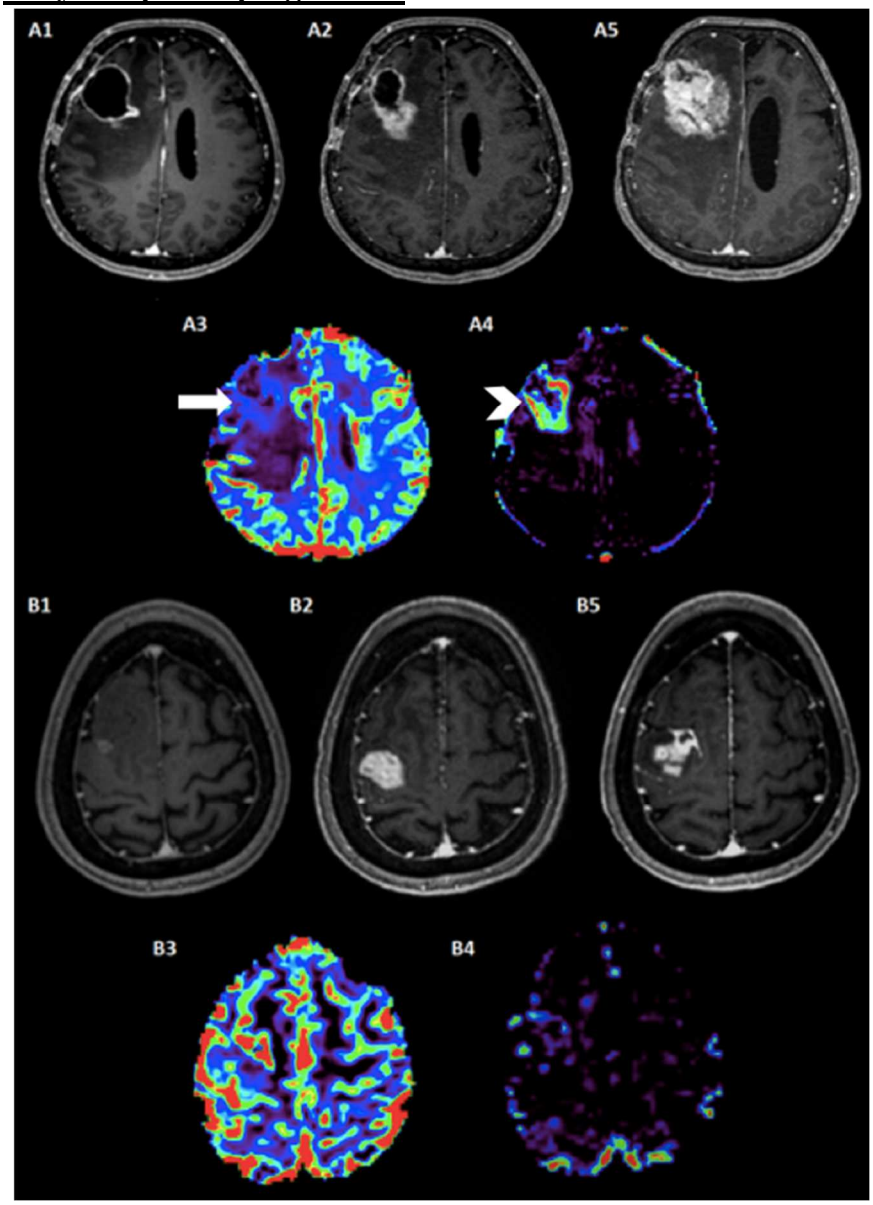

The top example demonstrates a case of early progression.

On post-radiochemotherapy T1-weighted MRI (A2), this 42-year old man presented a nodular enhancement on contact with post-surgical cavity not found on a previous T1-weighted MRI

performed before the radiochemotherapy (A1). This nodular enhancement exhibited slight elevation of CBV (A3, arrow) and a sharp increase of K2 (A4, arrowhead). On the follow-up T1-weighted MRI realized eight weeks later (A5), progression was indisputable.
The bottom example illustrates a case of pseudoprogression.
On a T1-weighted MRI performed two months after radiochemotherapy completion (B2), this 35-year old woman presented a major worsening of a right frontal enhancement comparatively to pre-radiochemotherapy T1 weighted MRI (B1). CBV map (B3) was difficult to analyze because of the proximity with cortical vessels. There was no obvious increase of K2 (B4). On the follow-up MRI performed 9 weeks later, this right frontal lesion decreased.

III.5. Table 2: Classification of patients with complete data according to their characteristics (rCBV≥ 1.75, rK2≥ 27 and *MGMT* promoter methylation).

		Pseudoprogression (n)	Early Progression (n)
MGMT methylated and rCBV < 1.75		4	0
MGMT methylated and rCBV > 1.75 or *MGMT* unmethylated and rCBV < 1.75	rK2< 27	2	3
	rK2≥ 27	1	7
MGMT unmethylated and rCBV high		0	16

Abbreviations: ROC: receiving operating characteristics, rCBV: relative Cerebral Blood Volume, rK2: relative K2.

III.6. Figure 4. Receiver operating characteristic curve of the combination of rCBV≥ 1.75, rK2≥ 27 and *MGMT* promoter methylation compared to those of rCBV≥ 1.75, rK2≥ 27 and *MGMT* promoter methylation.

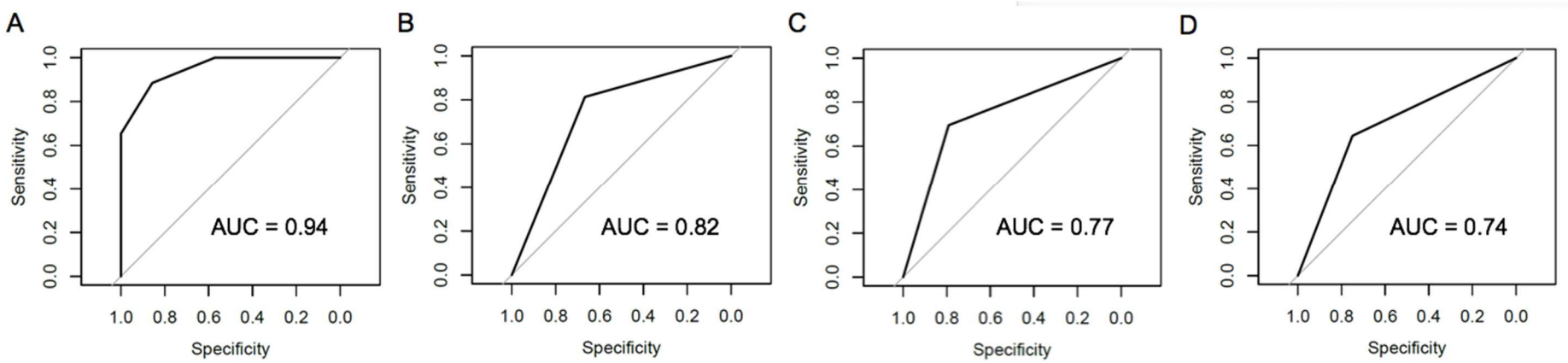

A: ROC curve of the combination of rCBV > 1.75, rK2 > 27 and *MGMT* promoter methylation.

B: ROC curve of rCBV≥1.75.

C: ROC curve of rK2≥ 27.

D: ROC curve of *MGMT* promoter methylation.

Diagonal line = 50% of the area under the receiver operating characteristic curve analyses.

Abbreviations: ROC= receiving operating characteristics, rCBV= relative Cerebral Blood Volume, rK2= relative K2, AUC= area under curve.

III.7. Table 3. Summary of the main characteristics associated with early progression and pseudoprogression in the present study and in comparison, with previous studies

	Sensitivity (%) in our study	Specificity (%) in our study	p-value*	Study	Year	Number of patients	Reported sensitivity (%)	Reported specificity (%)	p-value
Clinical Characteristics									
Neurological deterioration	52.5	79.2	0.013	W. Taal et al.[29]	2008	36 (18 EP, 18 Psp)	33	33	0.094
Conventional MRI									
New enhanced lesion	72.9	58.3	0.013	RJ Young et al.[6]	2011	97 (67 EP, 30 Psp)	40	49	0.380
Subependymal enhancement	55.9	75	0.015	R.-E. You et al[7]	2015	42 (24 EP, 18 Psp)	79.2	55.6	0.027**
				RJ Young et al.[6]	2011	97 (67 EP, 30 Psp)	38.1	93.3	0.003
Perfusion MRI									
rCBV≥ 1.75	92.3	71.4	0.002	M. Nasseri et al.[15]	2014	56(29 EP, 27 Psp)	100	100	< 0.001
				S. Gahramanov et al[13]	2013	19 (10 EP, 9 Psp)	100	100	0.004**
rK2≥ 27	76.9	85.7	0.005	NA	NA	NA	NA	NA	NA
Ktrans > 3.6	NA	NA	NA	AA. Thomas et al[16]	2015	37 (24 EP, 13 Psp)	69	79	NA
Molecular bio-markers									
Methylated *MGMT* promoter	81.8	72.3	< 0.001	Li H. et al[22]	2016	145 (38 EP, 38 Psp, 69 stable)	52.6	81.5	0.004**
				H. Motegi et al.[23]	2013	11 (8EP, 3PsP)	67	63	0.424
				Brandes et al.[24]	2008	50 (18 EP, 32 Psp)	66	89	0.0003**
*IDH*1 R132H mutation	9.1	100	0.096	Li H. et al.[22]	2016	145 (38 EP, 38 Psp, 69 stable)	66.7	100	0.0018**
				H. Motegi et al.[23]	2013	11 (8EP, 3Psp)	67	100	0.055

* Calculated using a Fischer exact test two-tailed.

** Data not presented in the original article and computed using a Fischer exact test two-tailed.

Abbreviations: NA= not available, rCBV= relative Cerebral Blood Volume, rK2= relative K2.

III.8 Performance of all analyzed parameters for the diagnosis of pseudoprogression (supplementary data).

	Sensitivity	Specificity	Accuracy	p*
Clinical characteristics				
Neurological deterioration	52.5 [39.1-65.7]	79.2 [57.9-92.9]	60.2% [48.9-70.8]	0.013
Conventional MRI characteristics				
New enhanced lesion	72.9% [59.7-83.6]	58.3% [36.6-77.9]	68.7% [57.6-78.4]	0.007
Marginal enhancement	72.5% [56.1-85.4]	30.2% [17.2-46.1]	50.6% [39.4-61.2]	0.787
Nodular enhancement	93.2% [83.5-98.1]	20.8% [7.1-42.2]	72.3% [61.4-81.2]	0.063
Callosal enhancement	33.9% [22.1-47.4]	79.2% [57.9-92.9]	46.9% [35.9-58.3]	0.245
Subependymal enhancement	55.9% [42.4-68.8]	75.0% [53.3-90.2]	61.5% [50.1-71.9]	0.010
Meningeal enhancement	42.4% [29.6-55.9]	62.5% [40.6-81.2]	48.2% [37.1-59.4]	0.687
Necrosis or cystic change	84.8% [73.0-92.8]	29.1% [12.6-51.1]	68.7% [57.6-78.4]	0.103
Increased of T2 peri-tumoral abnormality	88.1% [77.1-95.1]	25.0% [9.8-46.7]	69.9% [58.8-79.5]	0.139
Decrease of enhancement intensity	1.7% [0.05-9.1]	91.7% [73.0-98.9]	27.7% [18.5-38.6]	0.527
Increasing necrosis or cystic change	72.9% [59.7-83.6]	41.7% [22.1-63.4]	63.9% [52.6-74.1]	0.688
DSC-MRI characteristics				
rCBV≥ 1.75	92.3% [74.9-99.1]	71.4% [29.0-96.3]	82.1% [68.4-86.3]	< 0.001
rK2≥ 27	76.9% [56.4-91.1]	85.7% [42.1-99.6]	74.2% [69.1-80.3]	< 0.001
Molecular characteristics				
Methylated MGMT promoter	81.8% [59.7-94.8]	72.3% [58.3-84.1]	77.2% [67.5-87.2]	< 0.001
*IDH*1 R132H mutation	9.1 % [1.0-27.7%]	100% [85.8-100%]	8.3% [1.0-27%]	0.096
EGFR amplification	53.1% [34.7-70.9%]	63.6% [40.7-82.8%]	57.4% [43.2-70.8%]	0.940

* Calculated using a Fischer exact test two-tailed.